Nonequilibrium Processes

Deutsche Ausgabe: DOI: 10.1002/ange.201608367
Internationale Ausgabe: DOI: 10.1002/anie.201608367

Retrograde and Direct Wave Locomotion in a Photosensitive Self-Oscillating Gel

Lin Ren, Weibing She, Qingyu Gao, Changwei Pan, Chen Ji, and Irving R. Epstein**

Abstract: *Crawling motion mediated by retrograde and direct waves, that is, in the opposite or the same direction, respectively, as the muscular wave that generates it, is a fundamental mode of biological locomotion, from which more complex and sophisticated locomotion modes involving outgrowths such as limbs and wings may have evolved. A detailed general description of muscular wave locomotion and its relationship with other modes of locomotion is a challenging task. We employ a model of a photosensitive self-oscillating gel, in which chemical pulse waves and a stimulus-responsive medium play roles analogous to nerve pulses and deformable muscles in an animal, to generate retrograde and direct waves under non-uniform illumination. Analysis reveals that the directional locomotion arises from a force asymmetry that results in unequal translation lengths in the push and pull regions associated with a pulse wave. This asymmetry can be modulated by the kinetic parameters of the photosensitive Belousov–Zhabotinsky reaction and the performance parameters of the gel, enabling a transition between retrograde and direct wave locomotion.*

Motility, combined with directionality and collective behavior, plays an essential role in ensuring the survival of many organisms.[1,2] Crawling associated with muscular waves shares a common mechanism of mode switching with legged animals[3] and is a basic locomotion method that results from the mutual interaction of nervous signals, musculoskeletal deformation, and environmental factors. Retrograde and direct waves are generated by muscular waves that travel in the opposite and the same direction, respectively, as the locomotion of the animal.[4] Earthworms and limpets move by retrograde waves, whereas slugs and snails use direct waves. Polyplacophora can move by either retrograde or direct waves.[3] Previous researchers have proposed that the viscoelastic properties of mucus[5,6] play an important role in directed crawling, which is achieved through the interplay[7] between muscular wave propagation and the nonlinear hysteresis properties of mucus. However, fundamental questions still remain. For example, can retrograde and direct wave locomotion be directly obtained with a mechanistic model that does not assume nonlinear hysteresis viscoelasticity? What is the mechanistic role of anchoring (adhesion) segments and limbs in controlling the direction of muscular wave locomotion?

Active matter[8–11] is an integrated system whose constituent units consume energy to move or to do mechanical work. A widely studied form of artificial active matter is a self-oscillating polymer gel hosting the ruthenium-catalyzed Belousov–Zhabotinsky reaction (BZR).[12–14] As the BZR undergoes chemical oscillations, periodic changes in the redox state of the catalyst generate autonomous swelling and deswelling of the gel, converting chemical energy into mechanical force. Because the Ru-catalyst is photosensitive, the dynamic behavior of the gel can be modulated by light.[15] A model for such BZ gels, the gel lattice spring model (gLSM), has been developed by Balazs and co-workers.[16–18] It captures the large-scale shape changes and movement that occur in these gels.[19,20] However, key questions, for example, the control mechanism and details of the transition between retrograde and direct wave locomotion of the gel, remain unanswered.

Herein, we employ BZ waves and stimulus-responsive gels as analogues of the nerve pulses and deformable muscles, respectively, in an animal. We study gel locomotion under illumination by combining the gLSM[16–18] and a two-variable photosensitive Oregonator model that describes both photopromotion and photo-inhibition in the photosensitive BZR.[21–23] We identify two key factors of directional locomotion: periodic movements in muscles (or their analogues) and asymmetries in the interaction forces with the environment.[24] Spatially non-uniform illumination was used to modify the structure of waves in BZ gels, causing transitions between locomotion modes. Details of the model, patterns of illumination, parameters, and calculation procedures are given in Section 1 and Figure S1 of the Supporting Information.

Using the relationship between the nonmonotonic light intensity and the oscillation frequency of the photosensitive BZR (Figure S2a in the Supporting Information), we can design chemical waves driven by non-uniform illumination that propel the gel. In heterogeneous oscillatory BZ media coupled by mass transport, the waves with highest frequency dominate the direction of wave travel.[25–27] Figure 1 shows pulse waves excited by non-uniform illumination using the light intensities (I) highlighted in Figure S2a in the Supporting Information. Spatiotemporal plots of the concentration of the oxidized catalyst v ($I_{left} = I_A$, $I_{right} = I_B$, I_C and I_D) are shown

[*] L. Ren, W. She, Prof. Dr. Q. Gao, Dr. C. Pan, Dr. C. Ji
College of Chemical Engineering, China University of Mining and Technology
Xuzhou 221008 Jiangsu (P. R. China)
E-mail: gaoqy@cumt.edu.cn
Prof. Dr. I. R. Epstein
Department of Chemistry and Volen Center for Complex Systems, MS 015, Brandeis University
Waltham, 02454-9110 Massachusetts (USA)
E-mail: epstein@brandeis.edu
Supporting information and the ORCID identification number(s) for the author(s) of this article can be found under: http://dx.doi.org/10.1002/anie.201608367.

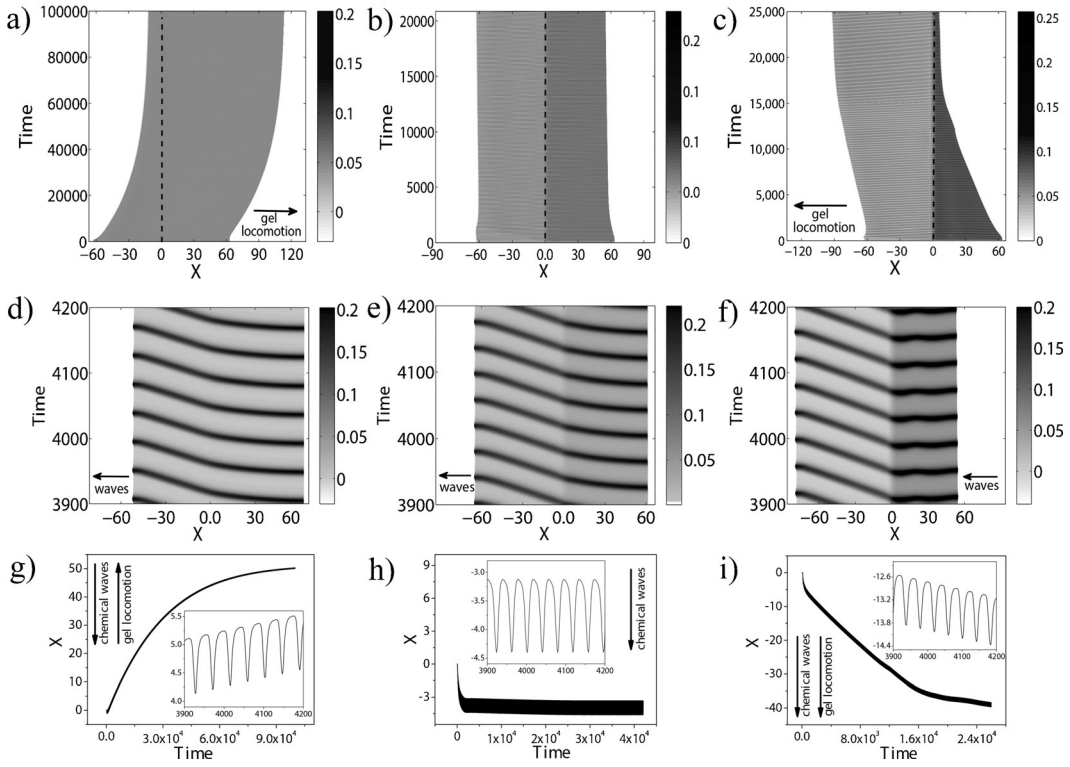

Figure 1. Spatiotemporal plots of ν and motion of gel center under non-uniform illumination. The three columns (from left to right) display retrograde wave locomotion, motionless state, and direct wave locomotion of gel at $I_{right} = I_B$, I_C, and I_D, respectively. a–c) Spatiotemporal plots of ν, d–f) expanded views of (a–c), g–h) position of gel center with time. $I_{left} = I_A$. Three movies showing gel movement can be found in the Supporting Information.

in Figures 1 a–c, respectively. All three scenarios have higher frequencies in the right half than in the left, so the waves travel from right to left (Figures 1 d–f). Under the action of these pulse waves, the autonomous swelling and de-swelling of the gel generates directional wormlike movement (Figures 1 g–i). When $I_{right} = I_B$, the gel moves along the $+x$ direction, opposite to the waves, indicating that retrograde wave locomotion occurs (Figures 1 a,d and g). When I_{right} is increased to I_C, the gel becomes motionless (Figures 1 b,e and h). Finally, when I_{right} is increased to I_D, the gel moves toward the $-x$ direction, showing direct wave locomotion (Figures 1 c,f, and i).

The motion of a BZ gel is controlled by its responsiveness to stimuli, the kinetics of the BZ waves, and the pattern of illumination. We characterize the motion by the quantity V_{gel}/V_{wave} to differentiate motion driven by retrograde waves and direct waves, where V_{gel} denotes the mean velocity of the gel's center and V_{wave} represents the velocity of the pulse waves. Thus, $V_{gel}/V_{wave} < 0$ indicates retrograde wave locomotion, whereas $V_{gel}/V_{wave} > 0$ indicates direct wave locomotion. Figure 2 a,b shows plots of V_{gel}/V_{wave} in the I_{left}–I_{right} and f–χ^* planes, which define the domains of retrograde and direct wave locomotion controlled by light intensity, and the parameters f and χ^*. Figure 2 a displays only the upper left triangular area, because all simulations were done with $I_{left} < I_{right}$. This map shows three regions, with direct wave locomotion occurring only in a narrow strip between line G ($V_{gel} = 0$) and line W ($V_{wave} = 0$). Along the vertical dashed line in Figure 2 a, V_{gel}/V_{wave} changes with I_{right} as shown in Figure S3 of the Supporting Information.

If the system displays synchronous dynamics, the movement of a single grid element can be used to analyze the gel movement. Figures 3 a–c show the position of the center grid point versus ∇v during one period. After one period, the net displacement toward or opposite to the direction of pulse propagation indicates retrograde or direct wave locomotion (Figures 3 a and c), respectively. When $I_{right} = 0.02815$, the critical value (Figure 3 b), the net displacement is zero. As seen in Figure 3 d, the negative region of the velocity curve grows more sharply than the positive region with $I_{right} > 0.02815$, which results in a transition from a net displacement (the time integration of the gel velocity over one period) toward the $+x$ axis to motion toward the $-x$ axis, that is, from retrograde to direct wave locomotion.

In the theory of 1D self-oscillating gels, the velocity of the polymer network is given by:[17]

$$V_p = \frac{\nabla\sigma}{\zeta'(\phi)} \tag{1}$$

where $\nabla\sigma = \nabla(\pi_{osm} - \sigma_{el}^{1D})$, $\zeta'(\phi) = \zeta(\phi)/(1-\phi)$, $\zeta(\phi) = \Lambda_0^{-1}(\phi/\phi_0)^{3/2}$, $V^{(p)}$ is the grid velocity of the gel, $\nabla\sigma$ is the stress gradient, and $\zeta'(\phi)$ is the apparent friction coefficient. As a plot of the stress gradient at the center grid point versus time (Figure 3 e) shows, the gel is successively subjected to the push and pull of the pulse wave during each

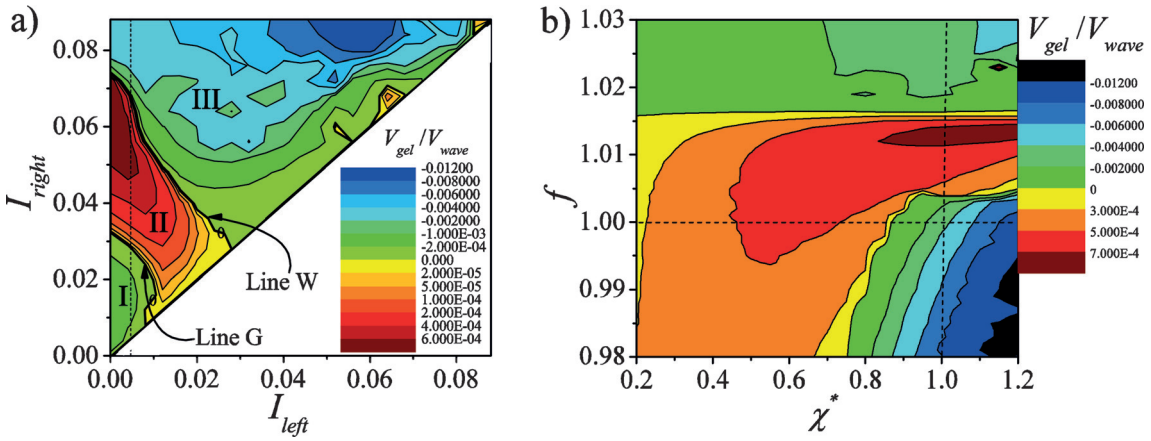

Figure 2. Effect of illumination intensity and kinetic and gel parameters on V_{gel}/V_{wave}. a) I_{left}–I_{right} plane. b) f–χ^* plane at $I_{left}=0.005$ and $I_{right}=0.05$. I, II, and III denote regions of retrograde, direct, and retrograde wave locomotion, respectively.

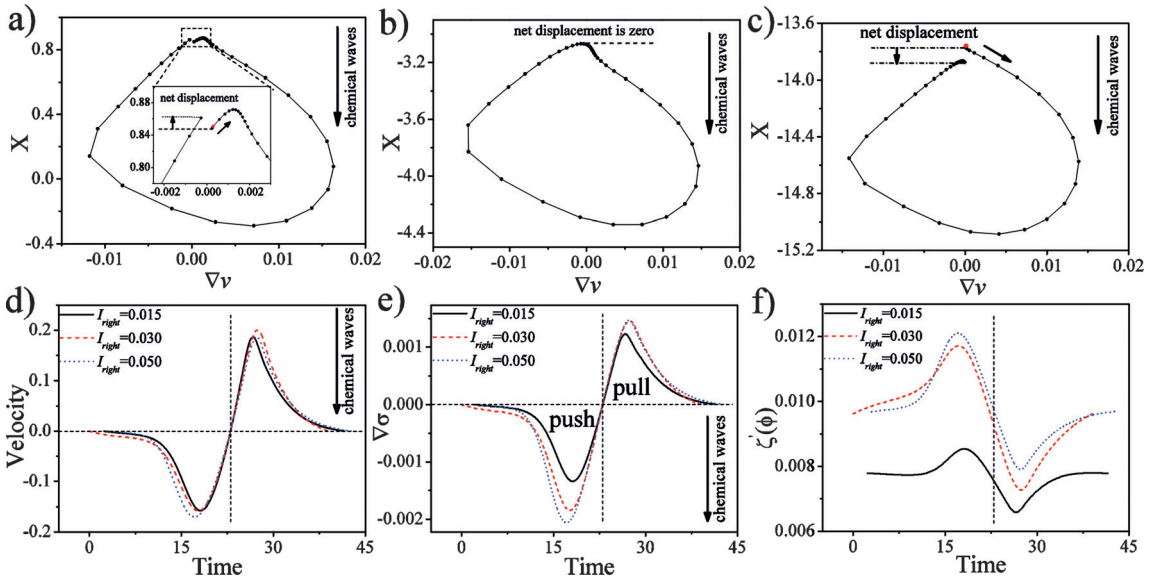

Figure 3. Position, velocity, stress gradient, and friction coefficient at the gel center in one oscillation period. a) $I_{right}=0.015$, b) $I_{right}=0.02815$, c) $I_{right}=0.050$. d),e) and f) Time evolution of grid velocity, stress gradient, and apparent friction. $I_{left}=0.005$.

cycle. Figure 3 f shows that the apparent friction coefficient between the polymer chain and the solvent is significantly greater in the push region than in the pull region, an effect that arises from a push-induced swelling and a pull-induced de-swelling of the volume fraction. According to the two-fluid model,[28] this process is accompanied by absorption and expulsion of the solvent in turn. Because the ratio between the stress gradient $\nabla\sigma$ and the apparent friction coefficient $\zeta'(\phi)$ gives the transient velocity of the grid element, $V^{(p)}$, the competition between $\nabla\sigma$ and $\zeta'(\phi)$ summed over the push and pull regions determines the net displacement of the gel.

As I_{right} is increased from 0.015 to 0.050, $|\nabla\sigma|$ grows more in the push region than in the pull region (Figure 3 e), always favoring generation of a direct wave. On the other hand, as shown in Figure 3 f, when I_{right} increases from 0.015 to 0.02815, the rise in the friction coefficient is also greater in the push region than that in pull region, which results in an initial enhancement of retrograde wave locomotion. However, as we continue to increase I_{right} from 0.02815 to 0.050, $\zeta'(\phi)$ changes relatively little during the push, whereas $\zeta'(\phi)$ continues to increase significantly in the pull region, which weakens the pull effect and leads to direct wave locomotion. The results of this analysis lead to the dynamic behavior depicted in Figure S3 of the Supporting Information.

To concisely express the net effect of the competition between $\nabla\sigma$ and $\zeta'(\phi)$, we use their extreme values to define a parameter ω that approximately replaces the time integration of $V^{(p)}$ over a cycle of motion

$$\omega = \kappa\left|\left[\frac{\nabla\sigma^{push}_{max}}{\zeta'_{max}(\phi)}\right]\Big/\left[\frac{\nabla\sigma^{pull}_{max}}{\zeta'_{min}(\phi)}\right]\right| \qquad (2)$$

where $\nabla\sigma^{push}_{max}$ and $\nabla\sigma^{pull}_{max}$ denote the extreme values of the stress gradient in the push or pull direction, respectively.

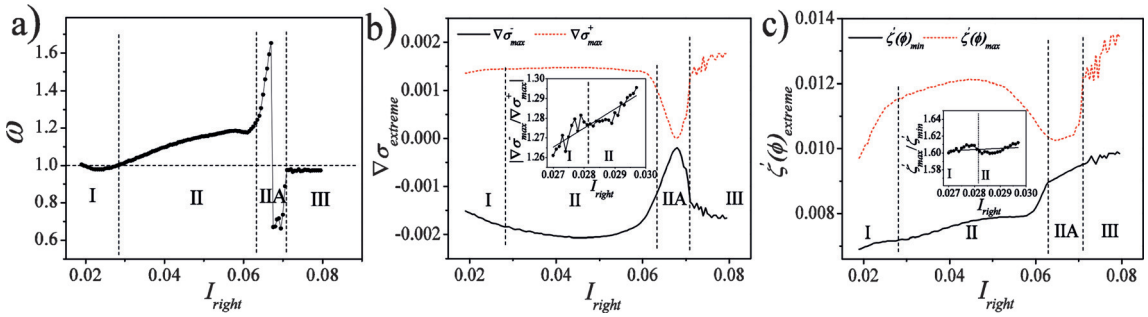

Figure 4. Effect of illumination intensity on kinematic parameters. a) ω vs. I_{right}. b) $\nabla\sigma^{-}_{max}$ and $\nabla\sigma^{+}_{max}$ *vs.* I_{right}. c) ζ' max and ζ' min vs. I_{right}. Large variations (IIA) between II and III arise from the nearly equal oscillation frequencies of the two illumination regions. $I_{left} = 0.005$.

$\zeta'_{max}(\phi)$ and $\zeta'_{min}(\phi)$, occurring at the same phase in the cycle as $\nabla\sigma^{push}_{max}$ and $\nabla\sigma^{pull}_{max}$, respectively, are the maximum and minimum values of the apparent friction coefficient. Below line W in Figure 2a, $\nabla\sigma^{push}_{max} = \nabla\sigma^{-}_{max}$ and $\nabla\sigma^{pull}_{max} = \nabla\sigma^{+}_{max}$, but above line W, $\nabla\sigma^{push}_{max} = \nabla\sigma^{+}_{max}$ and $\nabla\sigma^{pull}_{max} = \nabla\sigma^{-}_{max}$. This switch occurs as the propagation direction of the pulse wave reverses from the $-x$ to the $+x$ direction when I_{right} increases across line W. κ is chosen as 1.2578 to make $\omega = 1$ at the transition point ($I_{right} = 0.02815$). Thus, when $\omega > 1$, the push effect is dominant, resulting in direct waves; for $\omega < 1$, the pull effect wins, resulting in retrograde wave locomotion. As shown in Figure 4a, the value of ω indicates there are retrograde waves, direct waves, and retrograde waves in regions I, II, and III, respectively, in agreement with the V_{gel}/V_{wave} curve in Figure S3 of the Supporting Information. Detailed analysis (Section 4 of the Supporting Information) of Figures 4b,c indicates the key factor for transition across line G is the ratio of the maximum stress gradient between the push and pull regions, which results from wave asymmetry induced by the increased extreme catalyst concentration across the boundary under non-uniform illumination (Section 5, Figures S2b and S4–6 of the Supporting Information). The phase diagrams of the motion types in the f–χ^* plane (Figure 2b) are elucidated in Section 6 and Figures S7,8 of the Supporting Information.

Using a BZ self-oscillating gel as a model for studying crawling locomotion, we found that hysteretic viscoelasticity is not essential for directional locomotion, though it may play a major role in anchoring at different locations and slopes for gastropod locomotion.[5–7] Like the two-variable Oregonator, the FitzHugh–Nagumo model,[29–31] derived from the Hodgkin–Huxley model of neural action potentials,[32] produces pulse waves of potential. We anticipate that coupling the FitzHugh–Nagumo model with a muscle-like material should also result in directed locomotion.

Non-uniform spatial illumination across a boundary strengthens swelling and weakens de-swelling (Figure S5 in the Supporting Information), creating additional tension gradients (Section 5 of the Supporting Information), causing the transition from retrograde to direct wave locomotion depending on light intensity and other parameters such as f and χ^* (Figure 2). These effects resemble those of anchoring (adhesion) segments and appendages (such as limbs and wings) during cell migration and animal locomotion, which not only provide friction between the body and the substrate for stability of motion but also control the direction of locomotion by strengthening directed movement and/or inhibiting the opposite movement. For example, earthworms and the polychaete *polyphysia crassa* anchor to the ground during phases of contraction and expansion, promoting push and pull, respectively, to obtain retrograde and direct wave locomotion.[33,34] Even at the scale of a single cell, adhesion between the lamellipodium and the extracellar matrix, coupled to mechanical waves of lamellipodial actin, has been found to result in retrograde wave locomotion.[35,36]

Acknowledgements

This work was supported by Grant 21573282 from the National Natural Science Foundation of China, the Fundamental Research Funds for the Central Universities (No. 2015XKZD09), the Priority Academic Program Development of Jiangsu Higher Education Institutions (PAPD), the W.M. Keck Foundation and the U.S. National Science Foundation (CHE-1362477). We appreciate the help of Dr. V.V. Yashin on the gLSM.

Keywords: Belousov–Zhabotinsky reaction · direct waves · gels · locomotion · retrograde waves

How to cite: *Angew. Chem. Int. Ed.* **2016**, *55*, 14301–14305
Angew. Chem. **2016**, *128*, 14513–14517

[1] J. Gray, *Animal Locomotion*, Weidenfeld and Nicolson, London, UK, **1968**.
[2] R. M. Alexander, *Principles of Animal Locomotion*, Princeton University Press, Princeton, **2002**.
[3] S. Kuroda, I. Kunita, Y. Tanaka, A. Ishiguro, R. Kobayashi, T. Nakagaki, *J. R. Soc. Interface* **2014**, *11*, 20140205.
[4] R. H. Dubois, F. Vles, *C. R. Acad. Sci.* **1907**, *114*, 658–659.
[5] M. Denny, *Nature* **1980**, *285*, 160–161.
[6] R. H. Ewoldt, C. Clasen, A. E. Hosoi, G. H. Mckinley, *Soft Matter* **2007**, *3*, 634–643.
[7] M. Iwamoto, D. Ueyama, R. Kobayashi, *J. Theor. Biol.* **2014**, *353*, 133–141.
[8] D. Gonzalez-Rodriguez, K. Guevorkian, S. Douezan, F. Brochard-Wyart, *Science* **2012**, *338*, 910–917.
[9] S. Ramaswamy, *Annu. Rev. Condens. Matter Phys.* **2010**, *1*, 323–345.

[10] M. C. Marchetti, J. F. Joanny, S. Ramaswamy, T. B. Liverpool, J. Prost, M. Rao, R. AditiSimha, *Rev. Mod. Phys.* **2013**, *85*, 1143 – 1189.
[11] T. Vicsek, A. Zafeiris, *Phys. Rep.* **2012**, *517*, 71 – 140.
[12] A. N. Zaikin, A. M. Zhabotinsky, *Nature* **1970**, *225*, 535 – 537.
[13] R. Yoshida, T. Takahashi, T. Yamaguchi, H. Ichijo, *J. Am. Chem. Soc.* **1996**, *118*, 5134 – 5135.
[14] S. Maeda, Y. Hara, T. Sakai, R. Yoshida, S. Hashimoto, *Adv. Mater.* **2007**, *19*, 3480 – 3484.
[15] S. Shinohara, T. Seki, T. Sakai, R. Yoshida, Y. Takeoka, *Angew. Chem. Int. Ed.* **2008**, *47*, 9039 – 9043; *Angew. Chem.* **2008**, *120*, 9179 – 9183.
[16] V. V. Yashin, A. C. Balazs, *Macromolecules* **2006**, *39*, 2024 – 2026.
[17] V. V. Yashin, A. C. Balazs, *J. Chem. Phys.* **2007**, *126*, 124707.
[18] O. Kuksenok, V. V. Yashin, A. C. Balazs, *Phys. Rev. E* **2008**, *78*, 041406.
[19] V. V. Yashin, A. C. Balazs, *Science* **2006**, *314*, 798 – 801.
[20] P. Dayal, O. Kuksenok, A. C. Balazs, *Langmuir* **2009**, *25*, 4298 – 4301.
[21] T. Amemiya, T. Ohmori, M. Nakaiwa, T. Yamaguchi, *J. Phys. Chem. A* **1998**, *102*, 4537 – 4542.
[22] X. Lu, L. Ren, Q. Gao, Y. Zhao, S. Wang, J. Yang, I. R. Epstein, *Chem. Commun.* **2013**, *49*, 7690 – 7692.
[23] L. Ren, B. Fan, Q. Gao, Y. Zhao, H. Luo, Y. Xia, X. Lu, I. R. Epstein, *Chaos* **2015**, *25*, 064607.
[24] A. J. Ijspeert, *Science* **2014**, *346*, 196 – 203.
[25] A. S. Mikhailov, A. Engel, *Phys. Lett. A* **1986**, *117*, 257 – 260.
[26] B. Blasius, R. Tönjes, *Phys. Rev. Lett.* **2005**, *95*, 084101.
[27] O. U. Kheowan, E. Mihaliuk, B. Blasius, I. Sendina-Nadal, K. Showalter, *Phys. Rev. Lett.* **2007**, *98*, 074101.
[28] B. Barrière, L. Leibler, *J. Polym. Sci. Part B* **2003**, *41*, 166 – 182.
[29] R. FitzHugh, *Biophys. J.* **1961**, *1*, 445 – 466.
[30] J. Nagumo, S. Arimoto, S. Yoshizawa, *Proc. IRE* **1962**, *50*, 2061 – 2070.
[31] R. FitzHugh, *J. Appl. Physiol.* **1968**, *25*, 628 – 630.
[32] A. L. Hodgkin, A. F. Huxley, *J. Physiol.* **1952**, *117*, 500 – 544.
[33] J. Gray, H. W. Lissmann, *J. Exp. Biol.* **1938**, *15*, 506 – 517.
[34] H. Y. Elder, *J. Exp. Biol.* **1973**, *58*, 637 – 655.
[35] G. Giannone, B. J. Dubin-Thaler, O. Rossier, *Cell* **2007**, *128*, 561 – 575.
[36] J. Allard, A. Mogilner, *Cell Biol.* **2013**, *25*, 107 – 115.

Received: August 26, 2016
Published online: October 13, 2016

